ADC TECHNICAL REPORT 54-154

35

CRASH-SHOCK-ABSORBER LINK FOR AIRBORNE EQUIPMENT

CHARLES E. CREDE
RICHARD D. CAVANAUGH

THE BARRY CORPORATION

MARCH 1954

WRIGHT AIR DEVELOPMENT CENTER

AF-WP-(B)-O-18 JUL 54 75

NOTICES

When Government drawings, specifications, or other data are used for any purpose other than in connection with a definitely related Government procurement operation, the United States Government thereby incurs no responsibility nor any obligation whatsoever; and the fact that the Government may have formulated, furnished, or in any way supplied the said drawings, specifications, or other data, is not to be regarded by implication or otherwise as in any manner licensing the holder or any other person or corporation, or conveying any rights or permission to manufacture, use, or sell any patented invention that may in any way be related thereto.

The information furnished herewith is made available for study upon the understanding that the Government's proprietary interests in and relating thereto shall not be impaired. It is desired that the Judge Advocate (WCJ), Wright Air Development Center, Wright-Patterson Air Force Base, Ohio, be promptly notified of any apparent conflict between the Government's proprietary interests and those of others.

NOTICE: THIS DOCUMENT CONTAINS INFORMATION AFFECTING THE NATIONAL DEFENSE OF THE UNITED STATES WITHIN THE MEANING OF THE ESPIONAGE LAWS, TITLE 18, U.S.C., SECTIONS 793 and 794. THE TRANSMISSION OR THE REVELATION OF ITS CONTENTS IN ANY MANNER TO AN UNAUTHORIZED PERSON IS PROHIBITED BY LAW.

WADC TECHNICAL REPORT 54-154

CRASH-SHOCK-ABSORBER LINK FOR AIRBORNE EQUIPMENT

Charles E. Crede
Richard D. Cavanaugh

The Barry Corporation

March 1954

Electronic Components Laboratory
Contract No. AF33(600)-23113
RDO No. 111-27

Wright Air Development Center
Air Research and Development Command
United States Air Force
Wright-Patterson Air Force Base, Ohio

FOREWORD

This report was prepared by Charles E. Crede and Richard D. Cavanaugh of The Barry Corporation, Watertown, Massachusetts, on Air Force Contract No. AF 33(600)-23113 under RDO No. 111-27, "Aircraft Equipment Vibration and Shock Protection Devices." The work was administered under the direction of the Electronic Components Laboratory, Wright Air Development Center, with Mr. N. P. Kempton acting as project engineer.

Members of the engineering staff of The Barry Corporation principally engaged in this development are Charles E. Crede, Maurice Gertel, and Richard D. Cavanaugh.

ABSTRACT

Data on the final prototype model of a crash shock absorber link development are presented. The device retains electronic and other equipment installed in military aircraft and prevents such equipment from becoming missile. This precautionary measure is intended to prevent injury to personnel from loose equipment during crash conditions. The various elements of the device are described, and an analysis is presented of an extendible element with energy absorption capacity. This element is a helical spring adapted to be loaded in tension and made from heat treated material to withstand great strain. Results are presented as static force-deflection curves of the yielding spring and as oscillograms of acceleration as a function of time. Experimentally determined results are compared with the results of a theoretical analysis.

TABLE OF CONTENTS

LIST OF ILLUSTRATIONS

APPENDIX I

LIST OF ILLUSTRATIONS

APPENDIX II

INTRODUCTION

Experience in the operation of military aircraft over a period of years has shown that electronic and other accessory equipment installed in personnel spaces tend to become dislodged during crash conditions. Many of such crash conditions are not sufficiently severe to cause severe injury to personnel. Loose equipment within the personnel compartment is a hazard, however, and steps have been taken to prevent such equipment from becoming a missile. One of the solutions to this problem is the ruggedization of vibration isolators and mounting bases. This has been a satisfactory solution in many instances, although there is a tendency for weight to be added by such ruggedization. In other instances, the weight and outline dimensions of the equipment are such as to make ruggedization of the mounting base impractical. It is considered that a feasible solution in such instances would be the application of a crash shock absorber link to retain the equipment. Such a link would be secured at its opposite ends to the airframe and to the equipment under consideration. It would be intended to function as means to positively prevent the equipment from becoming a missile, and would further restrict its motion to a space not dangerous to nearby personnel.

I. DESIGN OF LINK

The essential elements of a crash shock absorber link for airborne equipment are (1) an extendible element capable of absorbing or dissipating considerable energy and (2) means to attach the opposite ends of such element to the airframe and to the equipment being restrained. Most of the time devoted to this development has been spent in the development, design and testing of the extendible element. The design of attaching means for the extendible link is largely within the province of maintenance and installation personnel.

One of the principal problems in attaching the extendible element to the equipment concerns the strength of the equipment. To maintain the weight of airborne equipment at a minimum, it is conventional practice to mount the components upon an adequately strong but somewhat compact chassis. The equipment is then housed within a relatively light dust cover. The structural members of the equipment thus tend to be inaccessible, while accessible parts of the equipment lack sufficient strength to exert an adequate restraining force upon the equipment.

Two suggestions for attaching the link to the equipment are illustrated in Figures 1 and 2. In Figure 1, a harness somewhat similar to that used for attaching a parachute to air delivered equipment is wrapped securely around the equipment. Such a harness includes a link at the intersection of the straps;

it is proposed to join this link with one end of the extendible element by means of standard galvanized steel aircraft wire. The other end of the extendible link would be attached to the airframe by a similar cable. In the suggestion illustrated in Figure 2, a U shaped member is attached to the equipment in the vicinity of the load carrying chassis. Such a link is adapted to be attached to the extendible element by a flexible cable as described with reference to Figure 1. The extendible element described in the following paragraphs is relatively short in its unextended position. Consequently, it can be adapted to a wide variety of installations by varying the lengths of the flexible cables attached to the opposite ends of the extendible element.

It seems evident that a wide variety of conditions will be encountered in a series of airplane crashes. To provide a criterion for the design of the crash shock absorber link, the Wright Air Development Center has made use of information obtained by its Aero Medical Laboratory. It has been specified that a link be capable of absorbing an amount of energy equivalent to that embodied in the velocity of the mounted equipment at the conclusion of a free fall of ten feet. This energy absorbing capacity is related to force and deflection by specifying a maximum deceleration of 17g as the motion of the equipment is arrested. This value is based upon known strengths of aircraft structural members. Extension of the link is limited to 12 inches during dissipation of this energy, as dictated by proximity of personnel. The specification for the Crash Shock Absorber Link may be defined graphically with reference to Figure 3 by stating that a curve of acceleration versus extension shall not exceed the bounds of the cross hatched area during conditions of a 10 foot free fall. It is a further requirement of this specification that substantially all of the energy embodied in the free fall be dissipated rather than stored so that the mounted equipment will be brought to rest as rapidly as possible.

It is characteristic of shock in general that expected levels of shock may be specified but that substantial overloads should be anticipated. It follows from this that the energy absorbing capacity of the link should not suddenly be limited during extension of the link; in other words, the force-deflection curve should exhibit gradual stiffening. Contractor has interpreted the specification applying to this development as requiring that the energy in a 10 foot free fall of the equipment be absorbed without the acceleration exceeding 17g or the extension exceeding 12 inches. If the energy required to be absorbed is greater than that embodied in a 10 foot free fall of the equipment, the maximum acceleration may exceed 17g or the maximum extension may exceed 12 inches. In any event, the characteristics should be such that the acceleration and extension proceed gradually in case of overload.

To establish a definition, a Crash Shock Absorber Link is hereby defined as an assembly of an extendible element with

appropriate flexible cables attached at either end. The extendible element is provided with loops at opposite ends adapted for attachement by pins to forks available from a stock of standard AN hardware. Such forks are adapted for ready attachment to flexible cables commonly used for aircraft purposes. The cables in turn may be adapted for attachment to the airframe structure and to the mounted equipment. It is preferred that at least one of the pinned connections include a quick disconnect device so that the mounted equipment can be removed from position without the use of tools.

The assembled Crash Shock Absorber Link is shown in Figure 4. It consists of the extendible element described in the preceding paragraph and flexible cables attached to opposite ends of the extendible element. The flexible cables are standard AN equipment, according to the specification set forth on Figure 4, and the forks are standard AN equipment also in accordance with the applicable specification set forth on Figure 4. The forks are swaged to the flexible cable by approved methods. The forks at the inner ends of the cables are attached to the extendible elements by standard AN bolts extending through the forks and through loops at the opposite ends of the extendible elements. A slight advantage in weight might be obtained by using AN pins here instead of the bolts specified. A photograph showing assembled Crash Shock Absorber Links in three sizes, together with extendible elements of three sizes after testing, is included as Figure 6.

The extendible element is the heart of the Crash Shock Absorber Link. After consideration of possible means to meet the requirements of development, Contractor concluded that the requirements of minimum weight and minimum size could best be met by the employment of a yielding metal structure. This takes the form of a tightly wound helical spring adapted to be loaded in tension through the end loops. The extendible element is shown in detail in Figure 5. It is made from high manganese steel of 0.55 to 0.75 percent carbon, ASTM No. A229-41 (SAE No. 1066), heat treated as set forth in Figure 5 for the various sizes of extendible link. It has been found that steel which is heat treated to the tensile strength and hardness indicated on Figure 5 is capable of sustaining the large plastic strains required in this application.

Steel which conforms to A229-41 is not inherently corrosion resistant and must be protected. Initial attempts at protection employed cadmium plating with a post plate treatment intended to eliminate hydrogen embrittlement. Such springs would not withstand without rupture an extension of the magnitude considered necessary for use as the extendible element in the crash shock absorber link. Consequently, prototypes of the links include

extendible elements protected by Seal-D 202 paint. This paint has been proved capable of withstanding salt spray tests normally required of airborne equipment.

Suggested methods for attaching the link to the airframe and to the equipment are set forth in Figures 7 and 8. As seen in Figure 4, the right hand end of the link is intended to be attached to the airframe. For this purpose, it is provided with an integral loop to engage the U bolt shown in Figure 8 which is designed to be bolted to the airframe structure. Referring to Figure 4, the left hand end of the Crash Shock Absorber Link is intended to be attached to the mounted equipment. The left hand end of the left hand cable is provided with a standard AN fork similar to that used at the inner ends of the cables. It is suggested that the bracket shown in Figure 7 be attached to the mounted equipment. Means for attaching the link to this bracket preferably embody a device adapted to be quickly disconnected without use of tools. A pin suitable for this purpose is available as a stock item from Aviation Development Inc., and bears their type number set forth in the table on Figure 4. These special pins have retractable detents which automatically retract upon insertion or removal of the pin. The U bolt arrangement shown in Figure 8 is suggested for use at one end of the link to allow greater freedom for angular orientation, thereby making it possible to install the link obliquely to the aircraft structure.

II. ANALYSIS

The deflection of a helical spring occurs by torsional strain of the wire constituting the spring. Even though the stress-strain curve for the spring material is generally somewhat irregular, it can be assumed with reasonable approximation that is has an inclined straight portion prior to yielding and a horizontal straight portion after yielding. With this assumed relation, it can be determined that the torque necessary to cause complete yielding of a round torsional member is 1/3 greater than the torque required to cause initial yielding of such a member[1]. The force-deflection curve for a yielding spring of very large spring index would thus have a final horizontal portion whose ordinate is 1/3 greater than the point of deviation from the inclined initial portion of the curve. For springs of relatively small diameter, however, the helix angle increases appreciably as the deflection takes place and the spring becomes stiffer.

The force-deflection relations in a helical spring deflected in tension beyond its yield stress have been investigated analytically, and the analysis is set forth in the Appendix. A family of force-deflection curves representing the properties of many springs are shown in Figure A-4 of the Appendix. These force-deflection curves are plotted to dimensionless parameters. The dimensionless force parameter is the actual force divided by a

hypothetical force P_i which is the force required to cause initial yielding of the wire in the spring. The dimensionless deflection parameter is the actual overall deflection of the spring divided by the developed length of wire around the helix. The parameter of the family of curves is $\tau_y C/G$, where τ_y is the yield stress in shear on the spring material, G is modulus of elasticity in shear, and C is the spring index or ratio of coil diameter to wire diameter.

Force-deflection curves as obtained experimentally from static tests of extendible elements in Sizes 1, 2, and 3 are shown in Figures 9, 10, and 11, respectively. Force-deflection curves obtained from the theoretical analysis are shown on the same sheets, converted to dimensional parameters to indicate the extent of the agreement with the experimentally determined curves. The degree of agreement between theoretical and experimental results is dependent largely upon the ability to predict the yield stress in shear of the spring material. It is difficult to predict this yield stress from the heat treatment or hardness of the spring material. It is equally difficult to determine the force at which initial yielding occurs, because this represents an infinitesimal change in the slope of the force-deflection curve.

The most feasible method of determining the yield stress of the material is to estimate the force at which complete yielding occurs. As indicated above, this occurs at a load 1/3 greater than the load at which initial yielding occurs. It is difficult to determine the force for complete yielding accurately, however, because the increasing helix angle causes the load to increase before the force-deflection curve would become substantially horizontal in the absence of an increasing helix angle. A force required for complete yielding can be estimated by noting the force at which the force-deflection curve tends to level off. From this force, the yield stress of the material may then be calculated by setting $P = 4/3 P_i$ following Equation (12) of the appendix and employing the spring dimensions set forth in Figure 5. The values of yield stress obtained in this manner are set forth in Figures 9 to 11 for the respective extendible elements. It is evident from the agreement between experimental and theoretical force-deflection curves, as set forth on Figures 9 to 11, inclusive that the theory of the yielding helical spring in tension is reasonably reliable if the yield stress in shear of the spring material is known.

III. WEIGHT

It is evident that weight is a very important consideration in airborne equipment. One of the initial ideas leading to development of the Crash Shock Absorber Link was that the weight embodied in the link may be less than the additional weight required to ruggedize isolators and mounting bases. A comparison of these weights is difficult to effect. In the first place,

only the Size 1 crash link, having a rated load of fifty pounds, is within the range of standard equipments whose weights are set forth in Specification MIL-C-172B. It is fairly common practice to construct equipment according to the general requirements of Specification MIL-C-172B, but embodying somewhat greater weights and larger dimensions. It is often the practice in such instances to employ stainless steel rather than aluminum for the structural members of mounting bases. Such bases tend to become relatively heavy, but there is no standard which calls for the use of stainless steel rather than aluminum. Even though a weight comparison tends to lack validity in all respects, some weights are given in Table I. The mounting base for the rated load of fifty pounds is constructed of aluminum in both ruggedized and non-ruggedized versions. In this instance, the saving in weight through the use of the crash link does not appear impressive. For the rated loads of 100 lbs. and 200 lbs., the ruggedized mounting bases are assumed to be constructed with stainless steel frames whereas the non-ruggedized mounting bases embody aluminum trays. The saving in weight made possible by use of the crash link in these instances may be substantial, principally because of the assumption that a stainless steel tray will be required.

Table I. Comparison of Weights

Rated Load Lb.	Typical Mounting Base Size	Weight of Crash Link Lb.	Weight of Mounting Base, Lb.	
			Ruggedized	Non-Ruggedized
50	B1-D	0.37	2.69	2.00
100	C1-D	0.87	5.41	3.12
200	C1-D	1.75	5.41	3.12

IV. DYNAMIC TEST

Dynamic tests of the Crash Shock Absorber Link were conducted, using the Type 20 Variable Impact Shock Machine. The set-up for conducting these tests is illustrated in Figure 12. The link is connected by means of a wire rope between the top of the elevator of the shock machine and the cross member forming the upper framework of the machine. The elevator is dropped in the conventional manner, and the slack in the cable connected to the link is such as to permit a free fall of the elevator of 9 feet before the load is applied to the link. The height of drop was limited to 9 feet by the height of the ceiling in Contractor's laboratory. It can be readily shown, however, that the results may be extrapolated to a ten foot free fall by noting that the spring force is substantially independent of deflection in the region of maximum deflection. Substantial additional deflection is possible without exceeding the limits of the cross-hatched area in Figure 3.

Results obtained from the dynamic tests consist primarily of records of elevator deceleration as a function of time, together with measurements of shock link extension at the conclusion of each drop. The deceleration was measured by a Statham Model A5A-500-2500 Accelerometer having a natural frequency greater than 1000 cycles per second and damping equal to 65 of critical. The instrumentation circuit is shown in Figure 13. The output from the accelerometer was amplified by a Techtronics Model 122 Pre-Amplifier and fed into a Dumont Model 322 Oscilloscope. The results were recorded by photographing the tube of the oscilloscope by a Dumont Polaroid Camera Model No. 297.

The exhibit which establishes the requirements for the Crash Shock Absorber Link specifies that the link shall have sufficient shock absorbing ability to absorb the energy embodied in a series of shocks or a single shock, equivalent to a free fall of the equipment of ten feet. To demonstrate compliance with this requirement and to show that the link has sufficient capacity to absorb the energy of a ten foot free fall, two links of each size were tested dynamically during final tests. In each size, one link was tested during two successive drops of five feet applied to the same link. A second link of the same size was then subjected to a single test involving a free fall of nine feet. All tests were conducted with the load on the shock line: i.e., the elevator weight plus added weight, equal to the rated load for the respective links.

The results of these drop tests are presented as acceleration-time curves, in the form of the oscillograms constituting Figure 14. The three oscillograms in this Figure refer to the three sizes of crash absorber link, as indicated on the Figure. The upper and middle traces on each oscillogram are the first and second five foot drops, respectively, of the first link of each size. The lower trace on each oscillogram represents a nine foot drop with rated load, using a different link than that employed for the first two successive five foot drops. Calibration of the traces is obtained by comparison with the calibration traces superimposed upon the test traces. All calibration traces have frequencies of 60 cycles per second and an amplitude calibration of 15g peak-to-peak.

The results of the dynamic tests are summarized in Table II. This table identifies the elements of each size which were subjected to dynamic tests, and indicates the height of drop for each element. Values of maximum acceleration as scaled from the oscillograms of Figure 14 are included in Table II. The maximum permanent deformation of each element at the conclusion of each drop is also set forth in Table II. To obtain a comparison between static and dynamic conditions the static force necessary to cause the observed maximum extension was taken from the static force-deflection curves of Figures 9 to 11, respectively, and recorded in Table II. Dividing this static force by the load in pounds supported by each element gives a maximum acceleration based on static tests, as set forth in the last column of Table II. A comparison of the acceleration values included in this column with the dynamically recorded values of acceleration indicates satisfactory agreement between static and dynamic tests.

Table II - Comparison of the Dynamic and Static Loads Developed by the Extendible Element

Size	Element Number	Drop No.	Ht. of Drop	Maximum Accel.	Extension of Spring After Drop #1	Extension of Spring After Drop #2	Static Force at Max. Defl.	Max. Accel. Based on Static Force
1	1	1	5 ft.	17.3g	3.3"			
1	1	2	5 ft.	14.1g		5.7"		
1	2	1	9 ft.	16.9g	5.8"		800 lb.	16g
2	1	1	5 ft.	16.3g	3.1"			
2	1	2	5 ft.	15.0g		5.6"		
2	2	1	9 ft.	17.2g	6.4"		1700 lb.	17g
3	1	1	5 ft.	15.0g	4.5"			
3	1	2	5 ft.	12.2g		7.9"		
3	2	1	9 ft.	15.0g	8.4"		2900 lb.	14.5g

Important features of the test results as set forth in Table II may be summarized as follows:

a. The maximum deceleration of the elevator in each instance was approximately 17g or less, subject to any qualifications imposed by accuracy of the instrumentation.

b. The maximum extension of each link at the conclusion of the test was substantially less than twelve inches. Element number two of each size was dropped from a height of only nine feet. The difference between extensions of such elements and the allowable extension of twelve inches suggests that the extension would have been well within limits if the drop had been from the specified height of ten feet.

c. The extension of each link after two five foot drops was substantially the same as the extension of an identical link after a single nine foot drop. This suggests that the extension is proportional to the energy absorbed, and that such energy may be absorbed in small increments with a result substantially equal to that obtained by absorbing the energy in a large increment.

It will be noted that the maximum acceleration transmitted by certain of the links is close to the maximum permitted acceleration of 17g. This is due to the unexpectedly high yield stress in shear obtained in the extendible elements. In some cases, this is as much as 50% greater than design values. The Crash Shock Absorber Links were purposely designed to have a yield load somewhat below the maximum acceptable, because the yield stress is difficult to predict from other properties of the material. Assuming the yield stress in shear to be known, the theory included in the Appendix is sufficiently complete to enable a designer to design a spring having any desired value of transmitted acceleration. Any desired compromise between weight and transmitted acceleration can then be made.

V CONCLUSIONS

The requirements for a Crash Shock Absorber Link for Airborne Equipment, as set forth in Exhibit WCES 52-44 dated 15 May 1952 may be met by employing a steel element adapted to yield upon application of excessive load. It is feasible to design such a yielding element similar to a helical spring adapted to carry a tension load. Such an element exerts a substantially constant force upon yielding several inches, then stiffens gradually as the helix angle increases so that optimum protection is provided in case of an overload beyond specification requirements.

It is feasible to design such a yielding helical spring on the basis of analytical work, employing known properties of the material. The design data made available as a result of the work reported here make it possible to design a yielding helical spring for any amount of energy absorption, transmitted acceleration and spring extension, provided the proper relations have been specified among these parameters.

VI REFERENCES

1. Timoshenko, S., Strength of Materials, D Van Nostrand Publishing Company, 2d ed., 1946, Chap. 8.

2. Wahl, A. M., Mechanical Springs, Penton Publishing Company, 1944, p.47.

3. Marks, Lionel S., Mechanical Engineers Handbook, McGraw-Hill, 5 ed., p 456.

4. Pierce, B. O., A Short Table of Integrals, Ginn and Company, Third Revised Edition, p. 91.

APPENDIX I

Analysis of a Yielding Helical Tension Spring

Symbol Index

a = radius of spring wire, in.

C = spring index, dimensionless

E = energy required to deflect spring, in. lb.

l = developed length of spring wire, in.

M_e = moment applied to wire by external force, in. lb.

M_I = resisting moment developed by a wire under torsion. in. lb.

N = number of coils in spring, dimensionless

P = axial force applied to spring, lb.

Q = energy required to deflect spring, dimensionless

R = radius of coil, in.

r = radial distances from center of wire to any element of wire cross section, in.

α = helix angle, radians

α_o = helix angle prior to deflection, radians

γ_y = shear strain at which yielding occurs, in/in.

δ = deflection of spring along its axis, in.

θ = total torsional displacement of wire of length l, radians

θ_o = torsional displacement per unit length of wire, radians

τ = shear stress, psi

τ_y = shear stress at which yielding occurs, psi

The expression for the resisting moment developed by a round wire stressed in torsion is

$$M_I = \int_0^a 2\pi \tau r^2 dr \qquad (1)$$

From Figure A-1, using the theory developed in reference 1,

$$M_I = \int_0^{\gamma_y l/\theta} 2\pi \frac{\tau_y \theta}{\gamma_y l} r \cdot r^2 dr + \int_{\gamma_y l/\theta}^a 2\pi \tau_y r^2 dr \qquad (2)$$

Integrating Equation (1) and combining terms:

$$M_I = \frac{2\pi \tau_y a^3}{3} - \pi \left(\frac{\gamma_y l}{\theta}\right)^3, \quad \left[\frac{\gamma_y l}{\theta} \leq a\right] \qquad (3)$$

When $\gamma_y l/\theta = a$, the shear stress area is triangular, having a maximum stress $G\theta a/l$ when $r = a$. Substituting in Equation (1):

$$M_I = \int_0^a 2\pi \left(\frac{G\theta r}{l}\right) r^2 dr = \frac{\pi G \theta a^4}{2l}, \quad \left[\frac{\gamma_y l}{\theta} \geq a\right] \qquad (4)$$

The equation relating angle of twist per unit length of the wire in a coil spring to the change in helix angle for a constant radius of coil is given by Wahl[1] as

$$\theta_o = \frac{\theta}{l} = \frac{\sin\alpha \cos\alpha}{r} - \frac{\sin\alpha_o \cos\alpha_o}{r} \qquad (5)$$

If α_o is assumed to be zero, this may be written

$$\frac{\theta}{l} = \frac{\sin\alpha \cos\alpha}{r} \qquad (6)$$

Referring to Figure A-2, the equation relating the angle θ , the deflection δ and the length l may be obtained from equation (6) by substituting

$$\frac{\delta}{l} = \sin\alpha, \quad \frac{\sqrt{l^2 - \delta^2}}{l} = \cos\alpha, \quad \frac{\sqrt{l^2 - \delta^2}}{2\pi N} = R \qquad (7)$$

Equation (6) then becomes

$$\frac{\theta}{l} = \frac{\delta}{l} \cdot \frac{\sqrt{l^2 - \delta^2}}{l} \cdot \frac{2\pi N}{\sqrt{l^2 - \delta^2}} = \frac{2\pi N \delta}{l^2} \qquad (7a)$$

Substituting $l = 2\pi R$ Equation (7a) becomes

$$\theta = \frac{\delta}{R} \tag{8}$$

It is desirable now to write Equation (3) in terms of spring deflection δ. Substituting from Equation (8) and noting from Figure A-1 that

$$M_I = \frac{2\pi\tau_y a^3}{3} - \frac{\pi\tau_y}{6}\left(\frac{\tau_y R}{G}\right)\left(\frac{l}{\delta}\right)^3 \tag{9}$$

The resisting moment defined by Equation (9) may be equated to the external or applied moment [2]:

$$M_e = PR \cdot \cos\alpha \tag{10}$$

Substituting expressions for R and cosine α as determined previously, and setting Equation (3) equal to Equation (10):

$$P = \frac{\sqrt{l^2-\delta^2}}{2\pi} \cdot \frac{\sqrt{l^2-\delta^2}}{2\pi} = \frac{2\pi\tau_y a^3}{3} - \frac{\pi\tau_y}{6}\left(\frac{\tau_y R}{G}\right)\left(\frac{l}{\delta}\right)^3 \tag{11}$$

Solving for P :

$$P = \frac{4\pi^2 l\tau_y}{3(l^2-\delta^2)}\left[a^3 - \frac{1}{4}\left(\frac{\tau_y R}{G}\right)\left(\frac{l}{\delta}\right)^3\right] \tag{12}$$

This expression for force P may be put into dimensionless form by dividing P by P_I, where $P_I = \pi\tau_y a^3/2R$ is the load at which the spring initially yields. Substituting the relation for the spring index $C = R/a$:

$$\frac{P}{P_I} = \frac{4}{3(1-\delta^2/l^2)} - \frac{1}{3}\left(\frac{\tau_y C}{G}\right)^3\left[\left(\frac{l}{\delta}\right)^3\left(\frac{1}{1-\delta^2/l^2}\right)\right] \qquad \left[\frac{\gamma l}{\theta} \geq a\right] \tag{13}$$

An expression for the force-deflection curve in dimensionless form for the interval $\gamma l/\theta \geq a$ a is obtained by first equating the external moment PR (for small values of α) to Equation (4)

$$PR = \frac{\pi G\theta a^4}{2l} \tag{14}$$

Solving Equation (14) for P, and dividing by the above expression for P_I :

$$\frac{P}{P_I} = \frac{\pi G\theta a^4}{2Rl} \times \frac{2R}{\pi\tau_y a^3} = \frac{G}{\tau_y C} \times \frac{\delta}{l} \qquad \left[\frac{\gamma l}{\theta} \geq a\right] \tag{15}$$

where $\delta = R\theta$ and $C = R/a$.

The dimensionless force-deflection curves, as given by Equations (13) and (15), are plotted in Figure A-4.

To obtain the energy absorbed by the spring for any value of deflection ratio δ/l , P/P_I must be integrated with respect to δ/l . Let Q represent the amount of energy absorbed by the

spring for a given deflection ratio δ/l, taken with reference to the energy absorbed by a spring deflecting a distance l with a constant force P_I:

$$Q = \int_0^{\delta/l} \frac{P}{P_I}\, d\left(\frac{\delta}{l}\right) \tag{16}$$

Substituting in Equation (16) the expressions for $\frac{P}{P_I}$ given by Equations (13) and (15):

$$Q = \int_0^{\frac{\delta_y}{l}} \frac{G}{C\tau_y}\left(\frac{\delta}{l}\right) d\left(\frac{\delta}{l}\right) + \frac{4}{3}\int_{\delta_y/l}^{\delta/l} \frac{d(\delta/l)}{(1-\delta^2/l^2)} - \frac{1}{3}\left(\frac{\tau_y C}{G}\right)^3 \int_0^{\delta/l} \left(\frac{l}{\delta}\right)^3 \frac{d(\delta/l)}{(1-\delta^2/l^2)} \tag{17}$$

The equation for the deflection of a helical spring when the stress is below the elastic limit is [3]

$$\delta = \frac{4\pi R^2 \tau_y N}{dG} \tag{18}$$

Substituting $C = \frac{2R}{d}$ and $l = 2\pi RN$ Equation (18) becomes

$$\delta/l = \tau C/G \tag{19}$$

The right side of Equation (19) is written $\frac{\tau_y C}{G}$ when the stress τ reaches the yield stress τ_y, and the deflection at which yielding occurs is designated δ_y. A new parameter $S = \tau_y C/G$ is now introduced, and therefore

$$\delta_y/l = S \tag{20}$$

Substituting from Equation (20) in Equation (15):

$$\delta/l = S\, P/P_I \tag{21}$$

Substituting from Equation (21) in Equation (17):

$$Q = \int_0^S \frac{1}{S}\left(\frac{\delta}{l}\right) d\left(\frac{\delta}{l}\right) + \frac{4}{3}\int_S^{\delta/l} \frac{d(\delta/l)}{(1-\delta^2/l^2)} - \frac{S^3}{3}\int_S^{\delta/l} \left(\frac{l}{\delta}\right)^3 \frac{d(\delta/l)}{(1-\delta^2/l^2)} \tag{22}$$

The term under the last integral in Equation (22) can be expanded to an infinite series which may be integrated term-by-term to give another infinite series, as indicated in the following expression:

$$Q = \frac{1}{2S}\cdot\frac{\delta^2}{l^2} + \frac{4}{3}\,\frac{1}{2}\ln\frac{(1+\delta/l)}{(1-\delta/l)}\Bigg|_S^{\delta/l} - \frac{S^3}{3}\left[-\frac{1}{2}\left(\frac{l}{\delta}\right)^2 + \ln\left(\frac{\delta}{l}\right) + \frac{1}{2}\left(\frac{\delta}{l}\right)^2 + \frac{1}{4}\left(\frac{\delta}{l}\right)^4 + \cdots\cdots + \frac{1}{2n}\left(\frac{\delta}{l}\right)^{2n}\right]_S^{\delta/l} \tag{23}$$

The series formed by all but the first two terms in the third integrand can be represented by the difference of the series formed by expanding $4\ln(1+\delta/l)$ and $\frac{1}{2}\ln\frac{(1+\delta/l)}{(1-\delta/l)}$ as follows:

$$\ln\left(1+\frac{\delta}{l}\right) = \frac{\delta}{l} - \frac{1}{2}\left(\frac{\delta}{l}\right)^2 + \frac{1}{3}\left(\frac{\delta}{l}\right)^3 - \frac{1}{4}\left(\frac{\delta}{l}\right)^4 + \cdots\cdots + (-)(-1)^n \frac{1}{n}\left(\frac{\delta}{l}\right)^n \quad (24)$$

$$\frac{1}{2}\ln\frac{(1+\delta/l)}{(1-\delta/l)} = \frac{\delta}{l} + \frac{1}{3}\left(\frac{\delta}{l}\right)^3 + \frac{1}{5}\left(\frac{\delta}{l}\right)^5 + \cdots\cdots\cdots\cdots + \frac{1}{2n-1}\left(\frac{\delta}{l}\right)^{2n-1} \quad (25)$$

Subtracting Equation (24) from Equation (25):

$$\frac{1}{2}\ln\frac{(1+\delta/l)}{(1-\delta/l)} - \ln(1+\delta/l) = \frac{1}{2}\left(\frac{\delta}{l}\right)^2 + \frac{1}{4}\left(\frac{\delta}{l}\right)^4 + \cdots\cdots\cdots + \frac{1}{2n}\left(\frac{\delta}{l}\right)^{2n} \quad (26)$$

The two logarithmic terms on the left hand side of Equation (26) can be substituted for the last several terms in Equation (23). Making this substitution, combining terms, and taking the limits indicated gives the following expression for Q :

$$Q = \frac{S}{3} + \frac{2}{3}\ln\frac{(1+\delta/l)}{(1-\delta/l)}\frac{(1-S)}{(1+S)} + \frac{S^3}{6}\left[\left(\frac{1}{\delta}\right)^2 - \ln\frac{(1+\delta/l)}{(1-\delta/l)}\frac{(1-S)}{(1+S)}\right] - \frac{S^3}{3}\left[\ln\frac{(1+S)}{(1-S)}\left(\frac{\delta}{l}\right)\frac{1}{S}\right] \quad (27)$$

It is evident from Equation (20) that S is always small relative to unity. Neglecting all powers of S greater than two, Equation (27) becomes

$$Q = \frac{S}{3} + \frac{2}{3}\ln\frac{(1+\delta/l)(1-S)}{(1-\delta/l)(1+S)} \quad (28)$$

Figure A-4 depicts this dimensionless energy relation. The expression for energy given by Equation (28) is dimensionless. It is made dimensional by multiplying by the load P_I for initial yielding and by the length l of the spring wire:

$$E = Q P_I l \quad (29)$$

Example:

It is required to design a yielding spring to transmit a load P for 2000 pounds and absorb 10,000 inch pounds of energy E with an extension δ of 6 inches or less.

To initiate the calculation, assume

$$\delta/l = 0.6$$

This defines Q and P/P_I from Figure A-4:

$$Q = \frac{E}{P_I l} = 0.91 \qquad \frac{P}{P_I} = 2.08 \qquad P_I = \frac{2000}{2.08} = 960^{\#}$$

The required length l of the spring wire is now found from Equation (29):

$$l = \frac{E}{P_I Q} = \frac{10,000}{960 \times 0.91} = 11.4"$$

From the above assumed value of δ/l ,

$$\delta = l \cdot \delta/l = 11.4 \times 0.6 = 6.84"$$

From the design objective P = 2000 lb. and the calculated relation

$$\frac{P}{P_I} = 2.08$$

$$P_I = 960 \text{ lb.}$$

Assuming τ_y = 80,000 psi and $C = 2R/d = 4$, the required wire diameter may be found from the relation:

$$P_I = \frac{\pi \tau_y d^3}{16R} = \frac{\pi \tau_y d^2}{8C}$$

solving for d:

$$d = \sqrt{\frac{8CP_I}{\pi \tau_y}} = \sqrt{\frac{8 \times 4 \times 960}{\pi}}$$

The number of coils can be found from l and R as follows:

$$N = \frac{l}{2\pi R} = \frac{l}{\pi C d} = \frac{11.4}{\pi \cdot 4 \cdot 0.35} = 2.6 \text{ turns.}$$

FIGURES FOR APPENDIX I

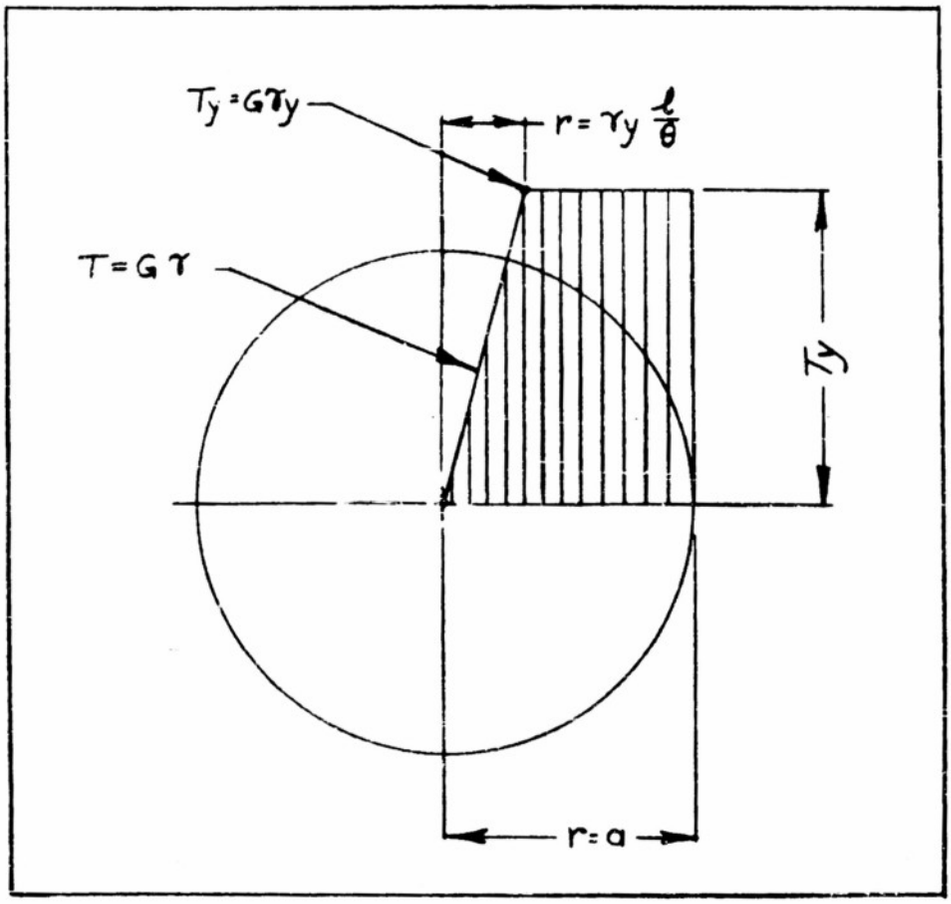

Figure 1. Distribution of Shear Stress on Wire Cross Section That is Beyond Yield Point of Fibers at Radius $r = \frac{S_y l}{\theta}$

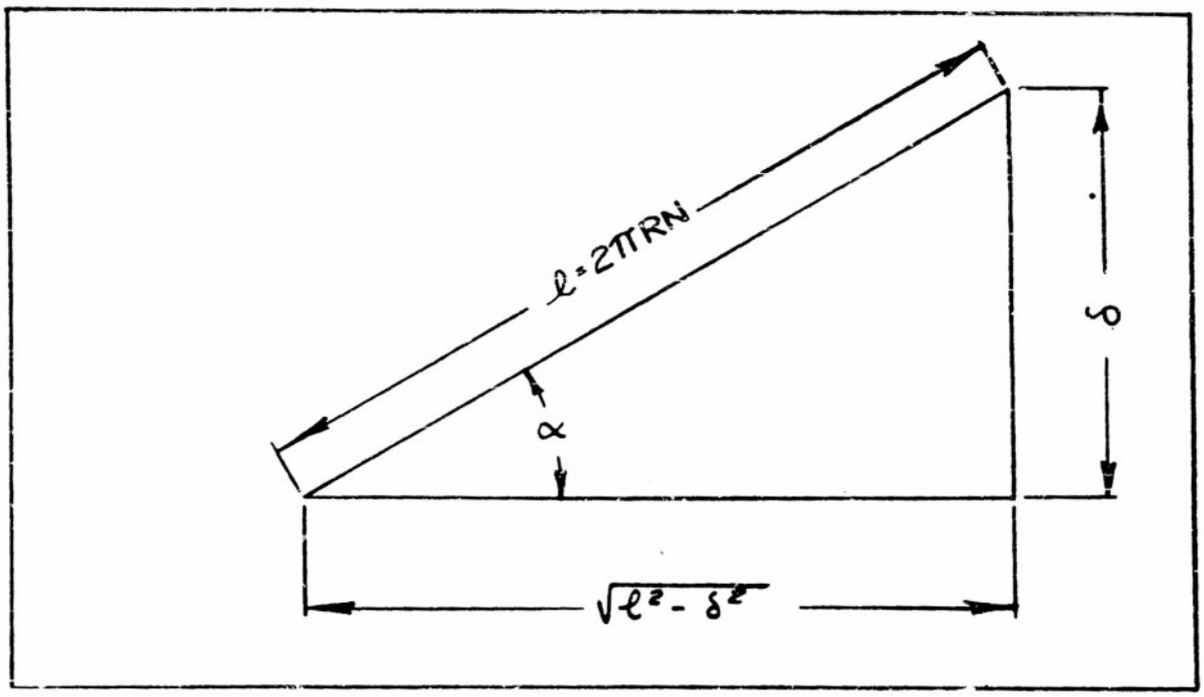

Developed Helix

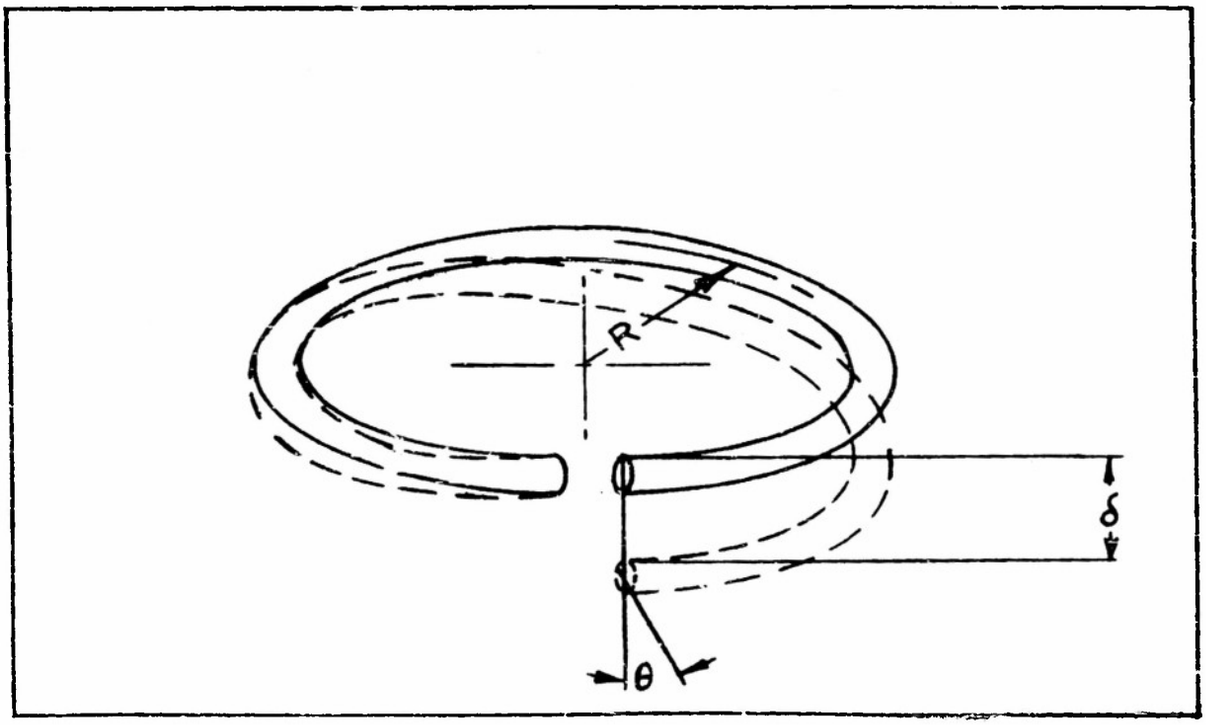

Figure 2. Geometric Representation of the Relationship Between Variables R, δ and θ

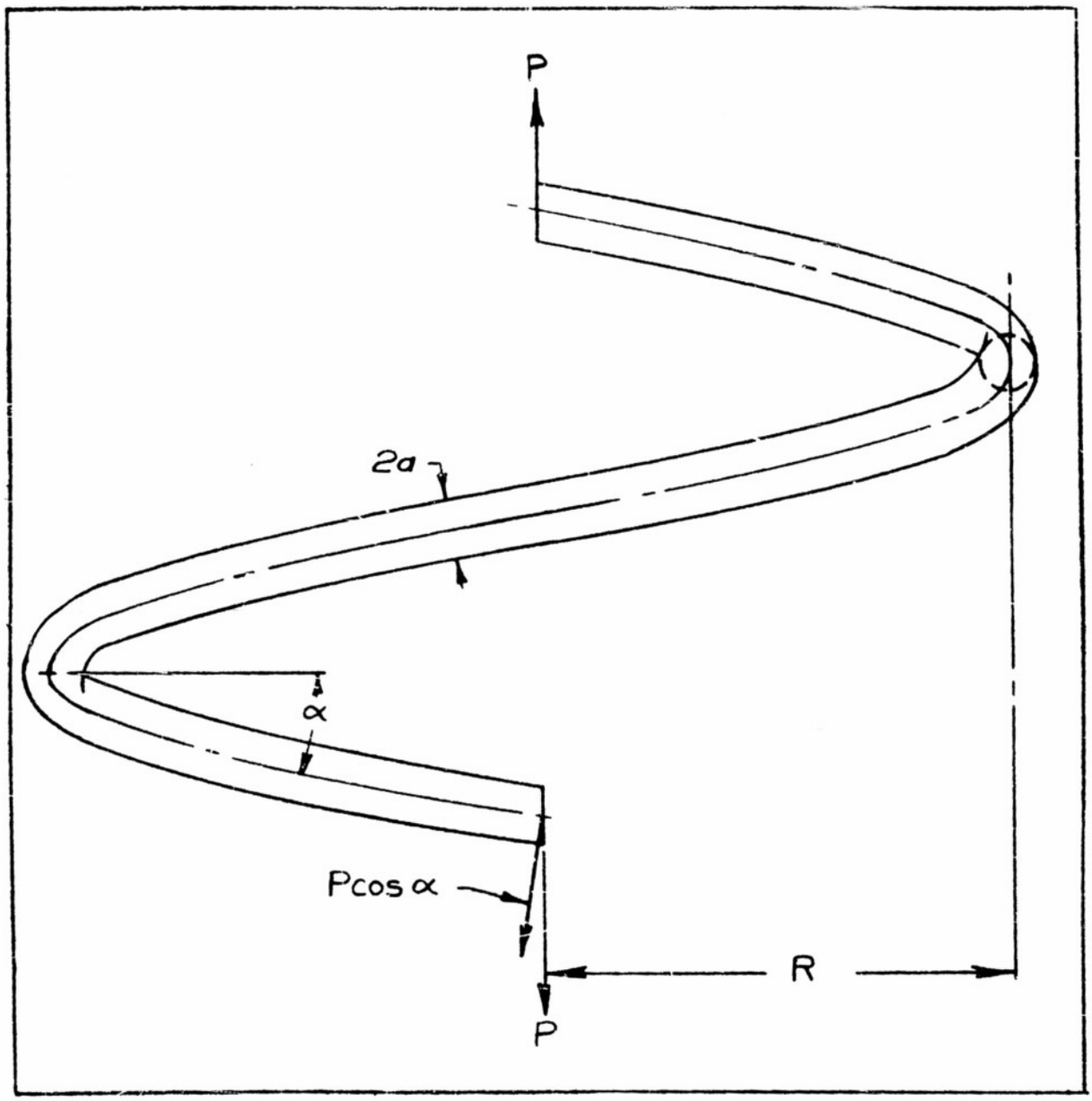

Figure 3. Twisting Moment Normal to Wire, $M_e = PR \cos \alpha$

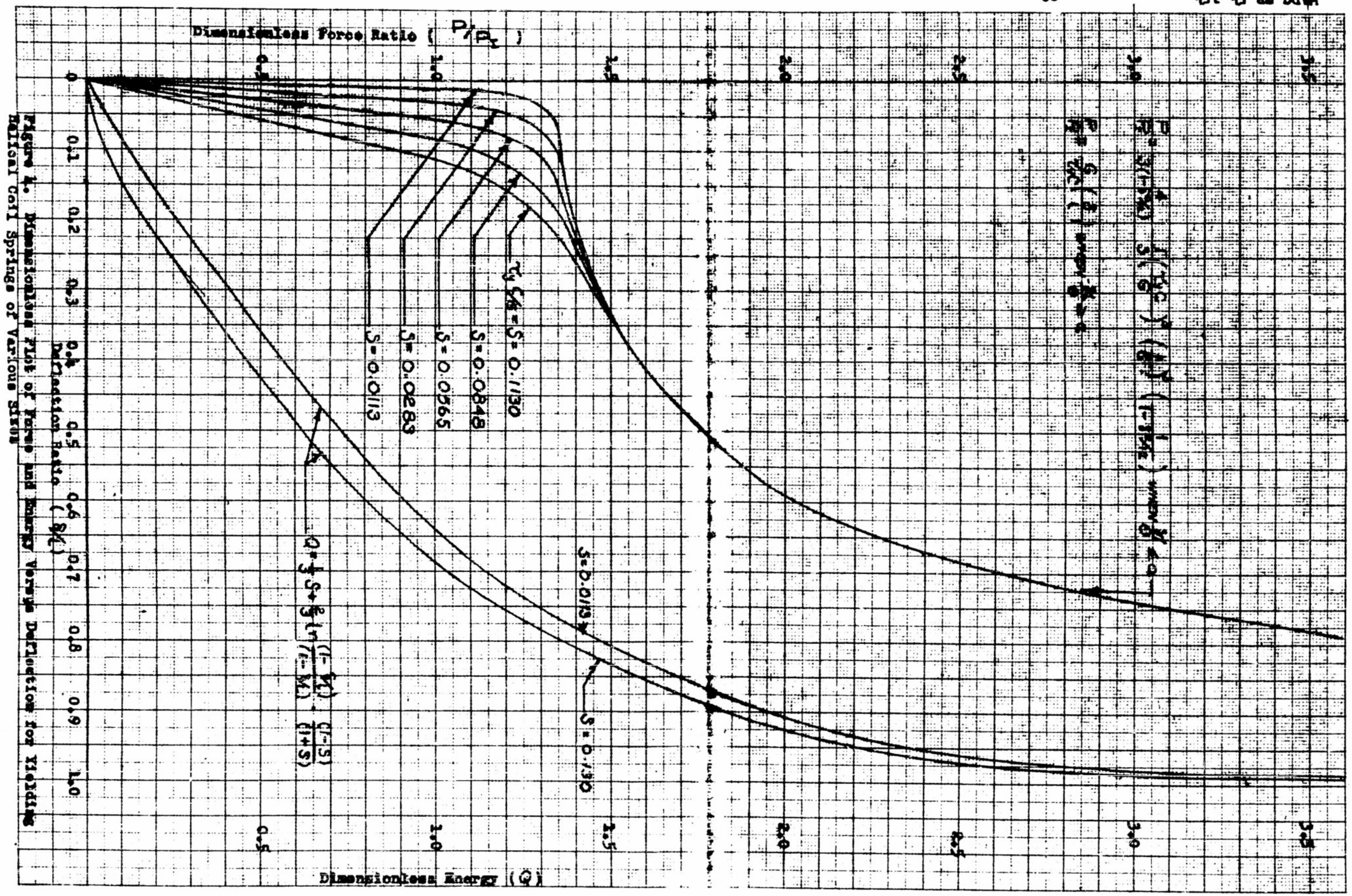

Figure 4. Dimensionless Plot of Force and Energy Versus Deflection for Variable Material Coil Springs of Various Sizes

Deflection Ratio (δ/δ_y)	0.6	0.7	0.8	0.9	1.0

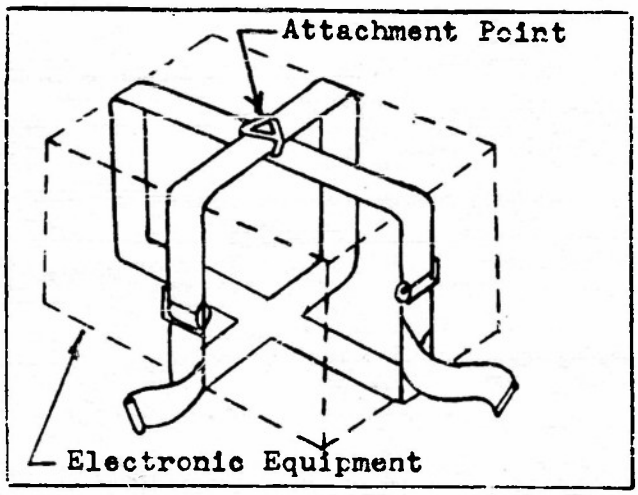

Figure 1. Suggested Means for Securing Crash Shock Absorbing Link to Electronic Equipment

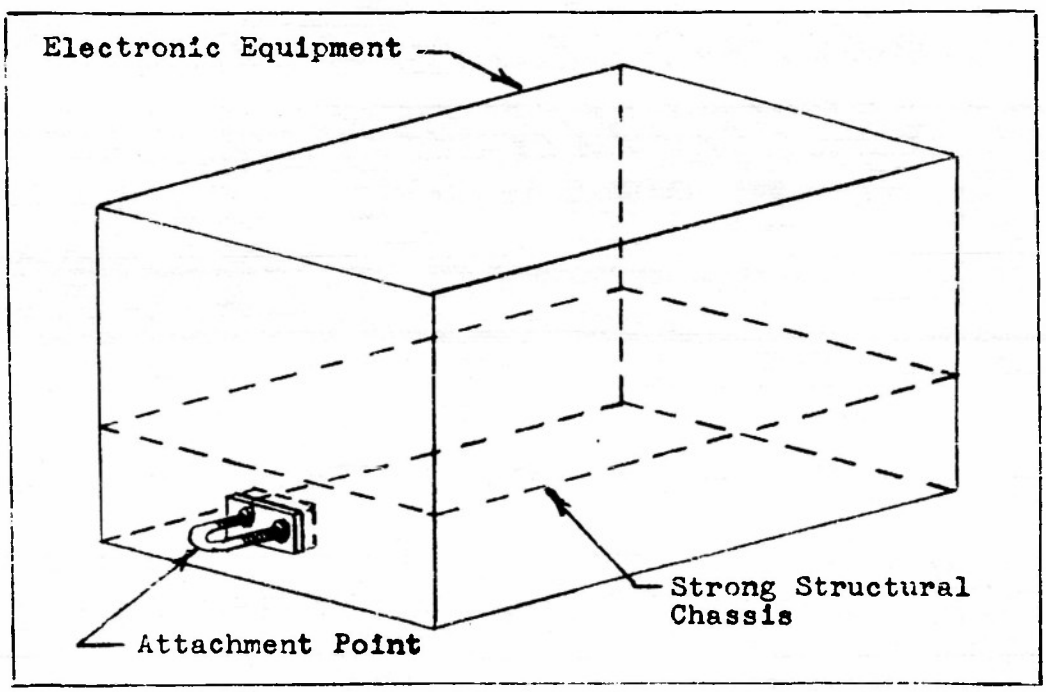

Figure 2. Suggested Means for Securing Crash Shock Absorbing Link to Electronic Equipment

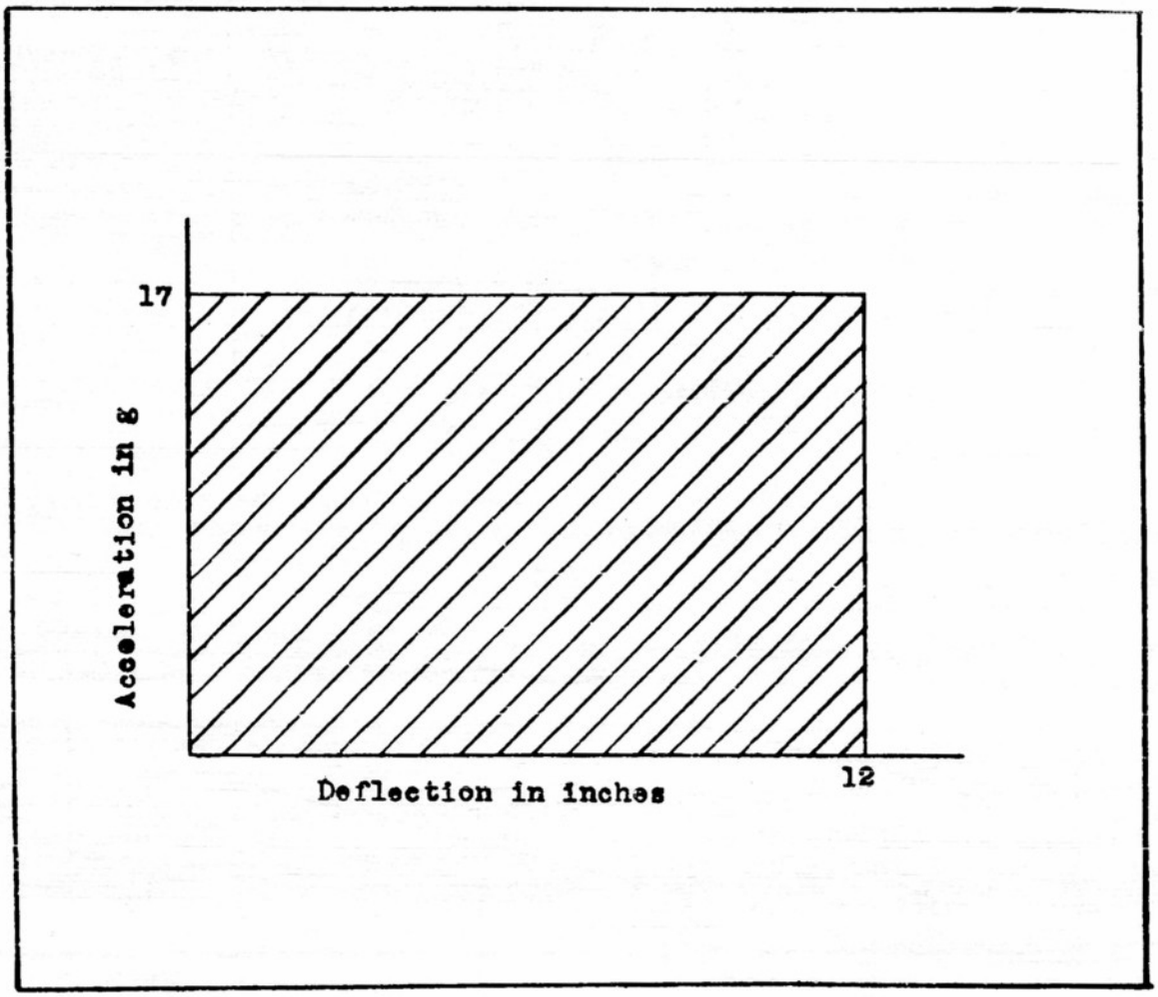

Figure 3. Area in Which Dynamic Load Deflection Curve Must Remain When Test Load is Subjected to 10 Foot Free Fall

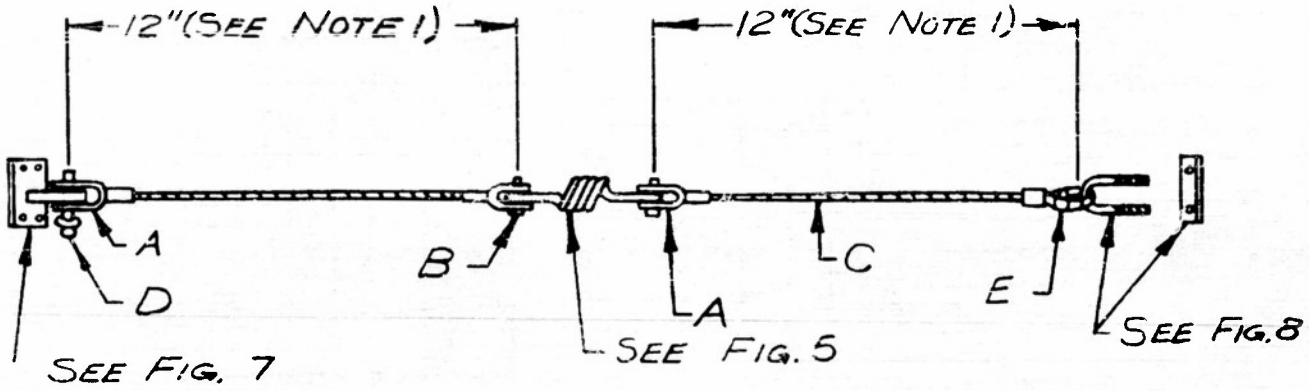

SIZE	RATED LOAD	A	B	C DIA. (NOTE 3)	D (NOTE 2)	E
1	50	AN667-4	AN105510 AN320-C3 AN381-2-6 AN960-C10L	1/8	A 305	AN100-4
2	100	AN667-6	AN105709 AN320-C5 AN381-2-10 AN 960-C516L	3/16	A507	AN100-6
3	200	AN667-8	AN105810 AN320-C6 AN381-3-12 AN960-C616L	1/4	A609	AN100-8

Note 1 - This dimension applies to prototypes furnished under the contract; may be modified to suit installation requirements.

Note 2 - Type number of Aviation Developments, Inc., 210 North Front Street, Burbank, California

Note 3 - Cable Specification AN-QQ-W-429

Figure 4. Assembly of Crash Shock Absorbing Link

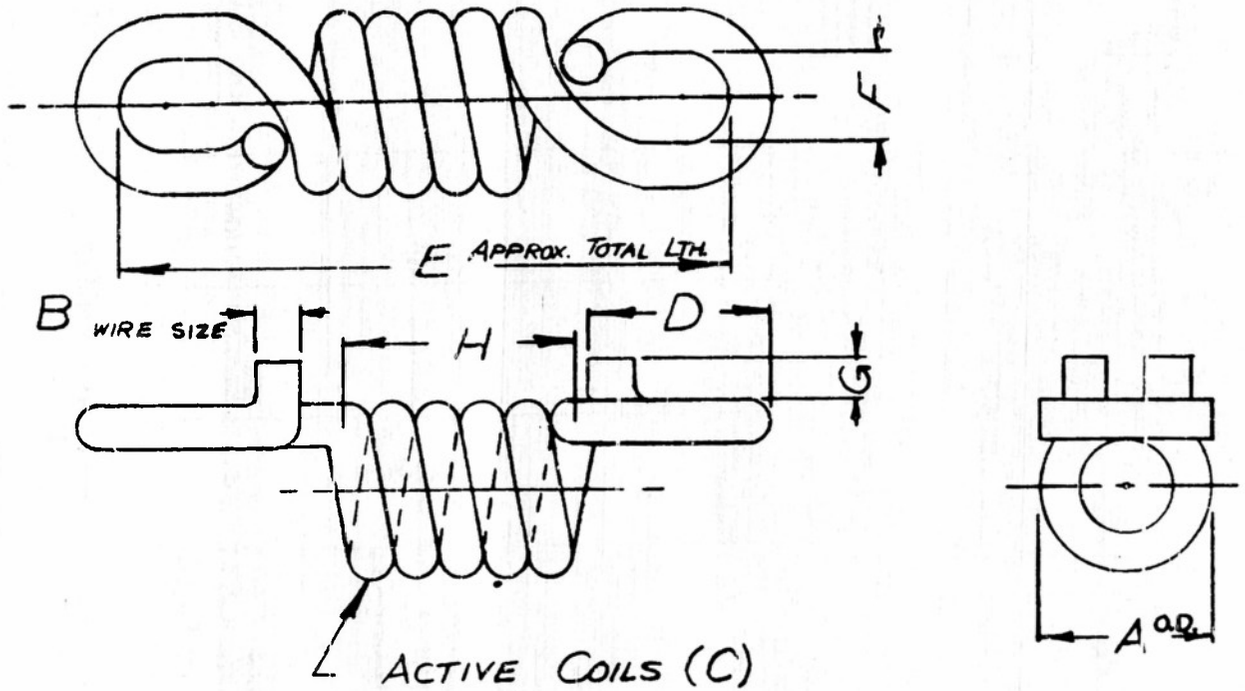

SIZE	RATED LOAD	A	B	C	D	E	F	G	H (REF)	ADDITIONAL MATERIAL REMARKS	TENSILE ULTIMATE STRENGTH (PSI)	ROCKWELL HARDNESS (C SCALE)	DEVELOPED LENGTH (ACTIVE COILS)
1	50	$\frac{13}{16}$	0.177	$5\frac{1}{2}$	$\frac{23}{32}$	$2\frac{1}{8}$	$\frac{3}{16}$	$\frac{3}{8}$	0.97	COMPOSITION A	180,000	35	11.00
2	100	$1\frac{1}{8}$	0.250	5	$1\frac{1}{16}$	3	$\frac{5}{16}$	$\frac{1}{2}$	1.25	COMPOSITION			13.75
3	200	$1\frac{7}{16}$	0.312	4	$1\frac{7}{16}$	$3\frac{1}{2}$	$\frac{7}{16}$	$\frac{5}{8}$	1.25	B	160,000	32	14.16

Notes: 1. Material - Oil Tempered Spring Wire (ASTM A229-41) See Table For Composition
2. Stress Relieve
3. Heat Treat See Table

Figure 5. Extendible Element

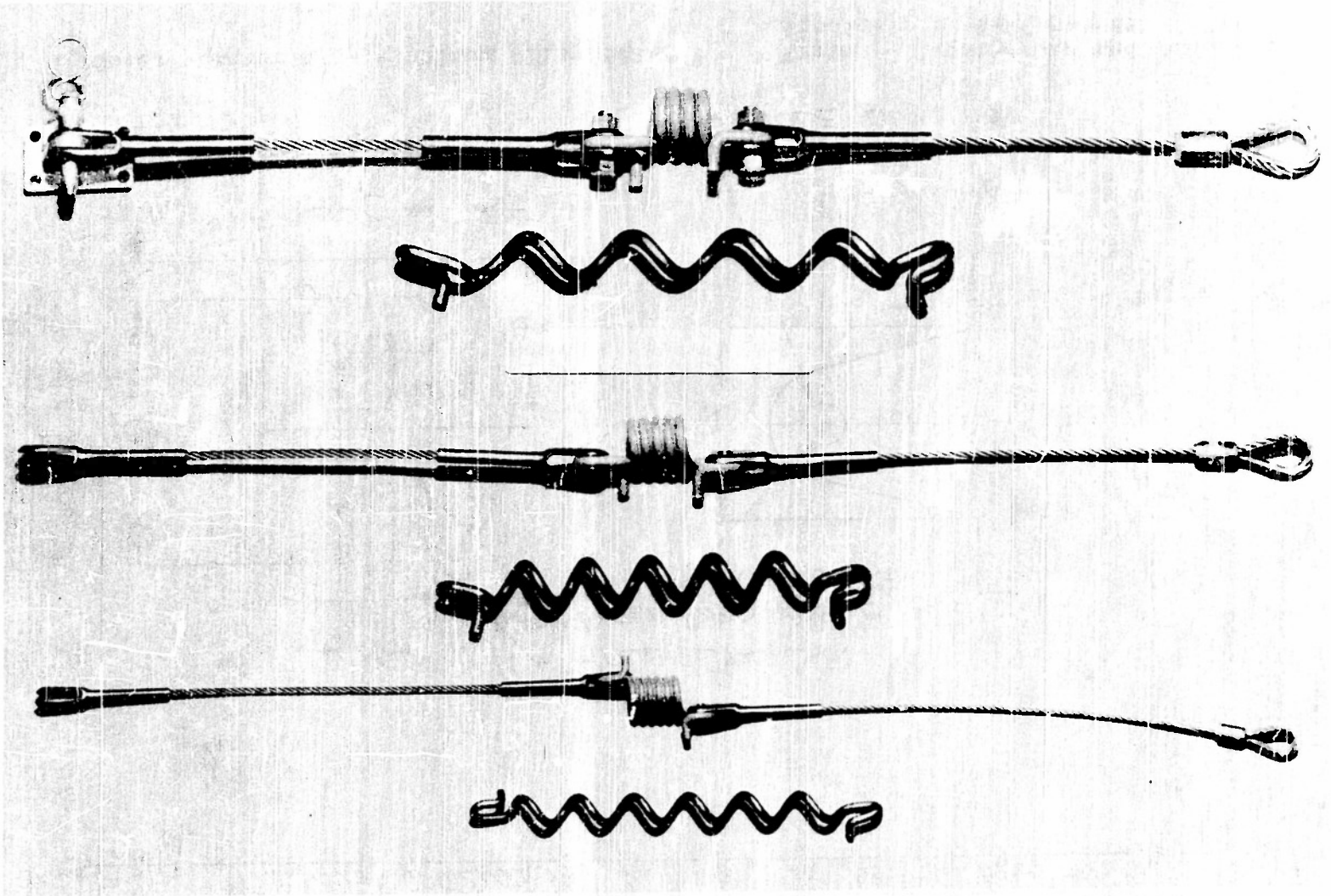

Figure 6. The Three Sizes of Crash Shock Absorbing Links Before and After Extension

SIZE	A	B	C	D	E	F	G	H	J	K	L	M
1	1	1 1/2	.500	1.000	1/4	1/4	1/4	3/4	5/8	1/8	.173	3/16
2	1 1/4	2	.750	1.500	1/4	1/4	3/8	1 1/4	3/4	3/16	.201	5/16
3	1 1/2	2 1/2	1.000	2.000	1/4	1/4	1/2	1 3/4	7/8	1/4	.266	3/8

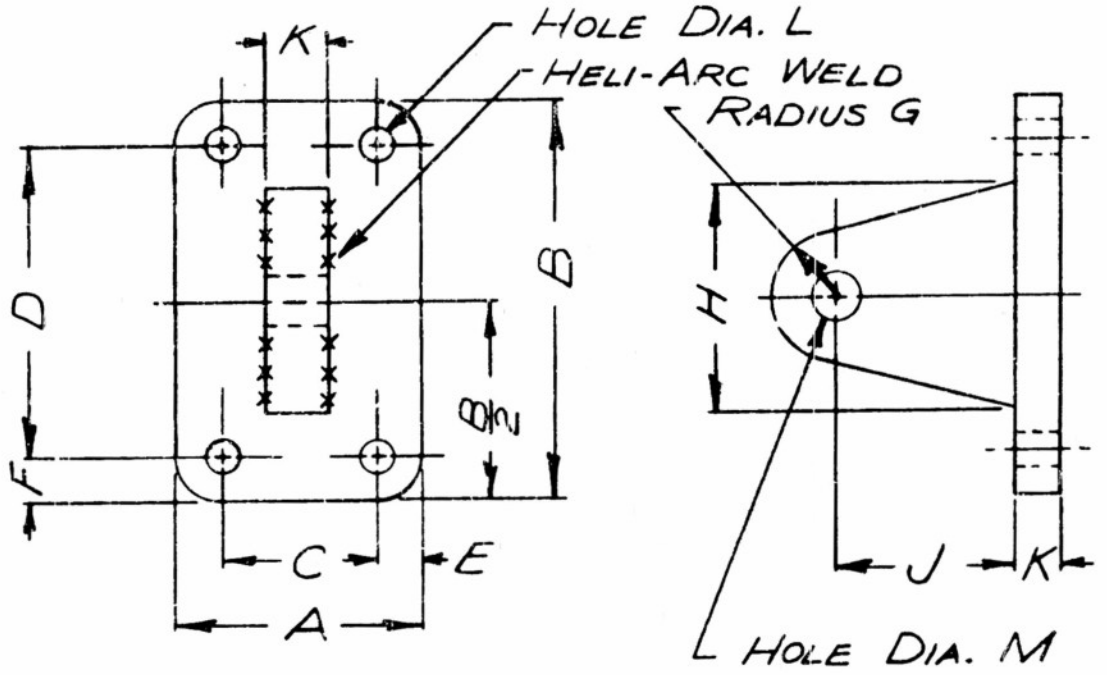

Note: Material - Aluminum Alloy 52S-H32 Finish - Caustic Dip and Dull Clear Anodize per AN-QQ-A-696a

Figure 7. End Attachment

SIZE	A	B	C	D	E	F	G	H	J	K	L
1	1 1/2	5/8	1/8	1	1/4	#3-40 NC-2	1 1/4	3/8	3/16	1/16	5/16
2	1 3/4	11/16	3/16	1 1/8	1/4	#5-32 NC-2	1 1/2	9/16	9/32	1/8	13/32
3	2	3/4	1/4	1 1/4	1/4	1/4-20 NC-2	1 3/4	3/4	3/8	3/16	1/2

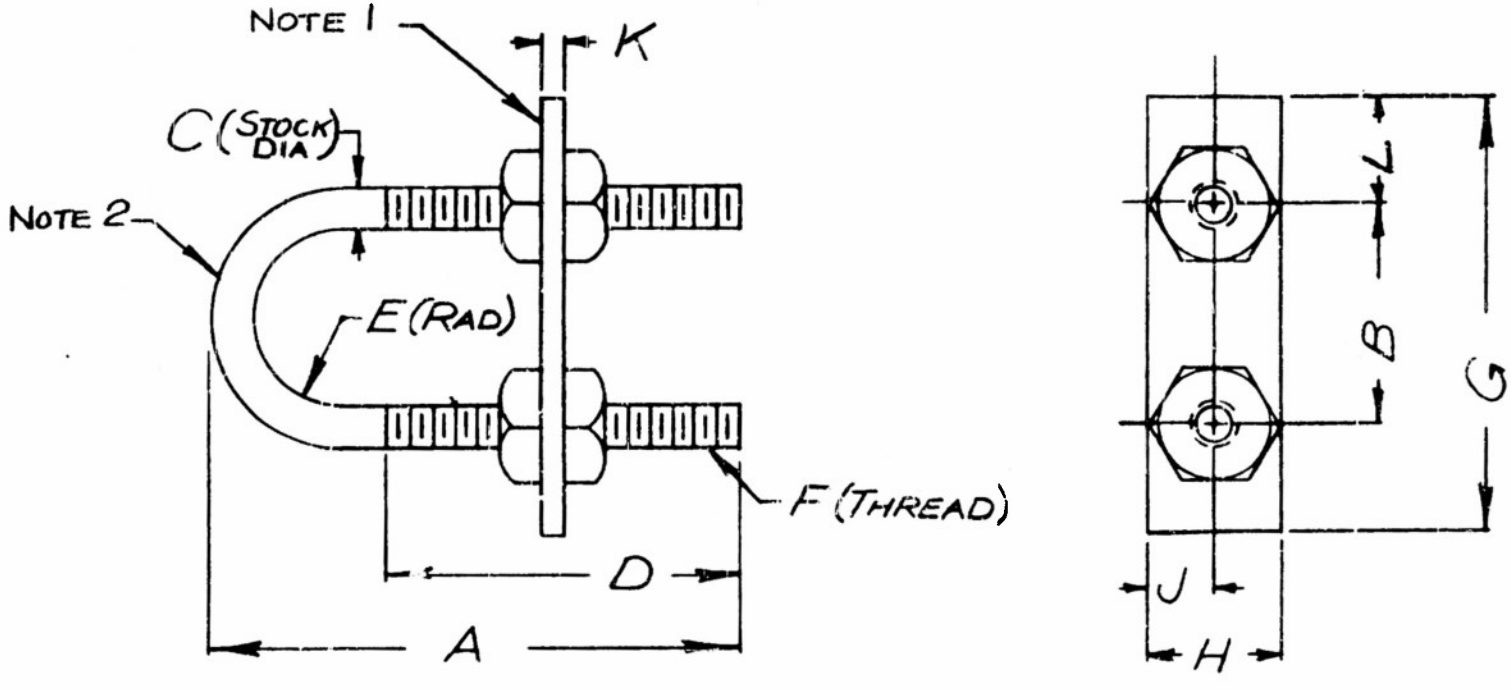

Note: 1. Material - Aluminum Alloy 52S-H32 Finish - Caustic Dip and Dull Clear Anodize per AN-QQ-A-696a

2. Material - Stainless Steel, AISI 303 Finish - Passivate

Figure 8 . End Attachment

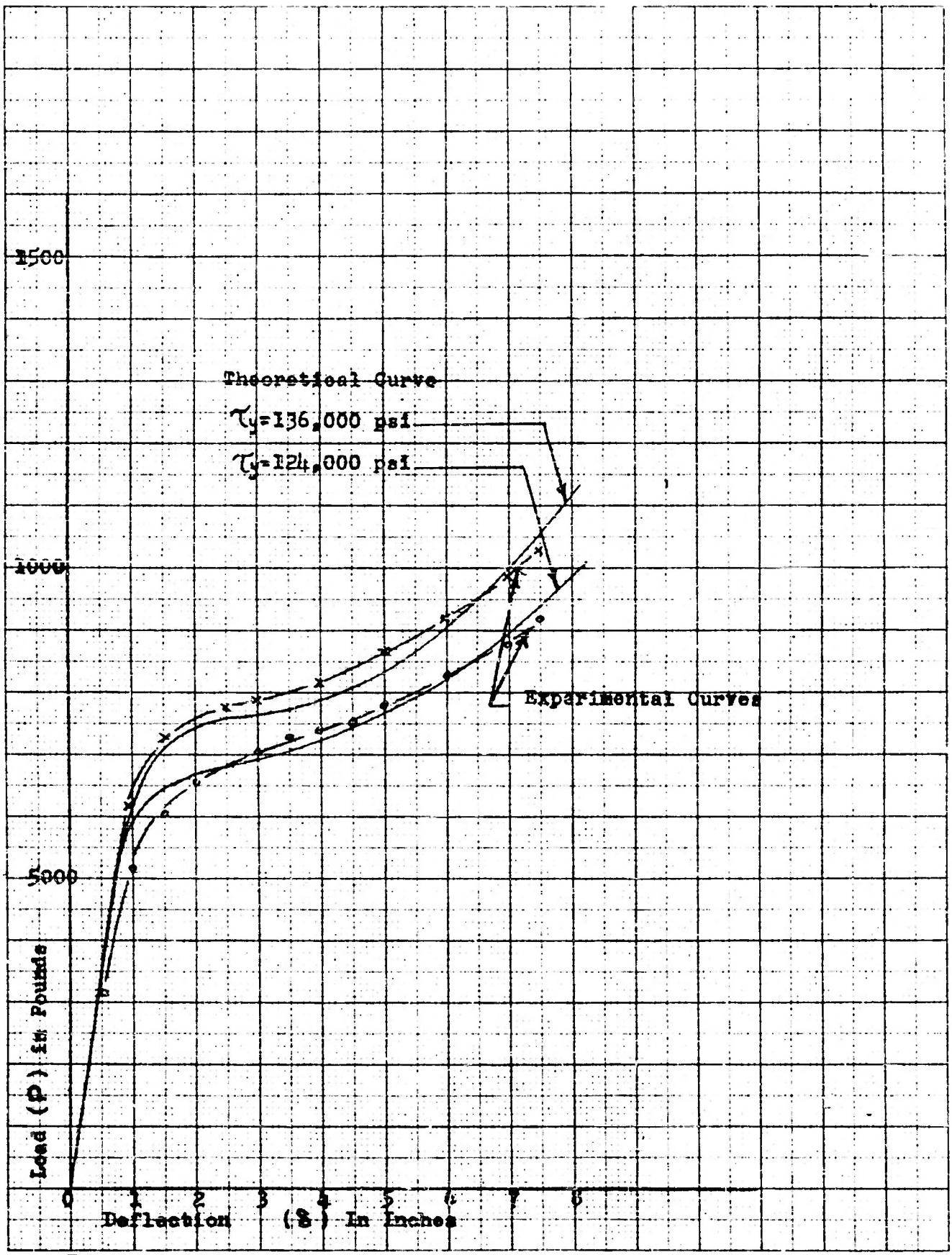

Figure 9. Comparison of Experimental and Theoretical Load-Deflection Curves of the Size 1 Extendible Element

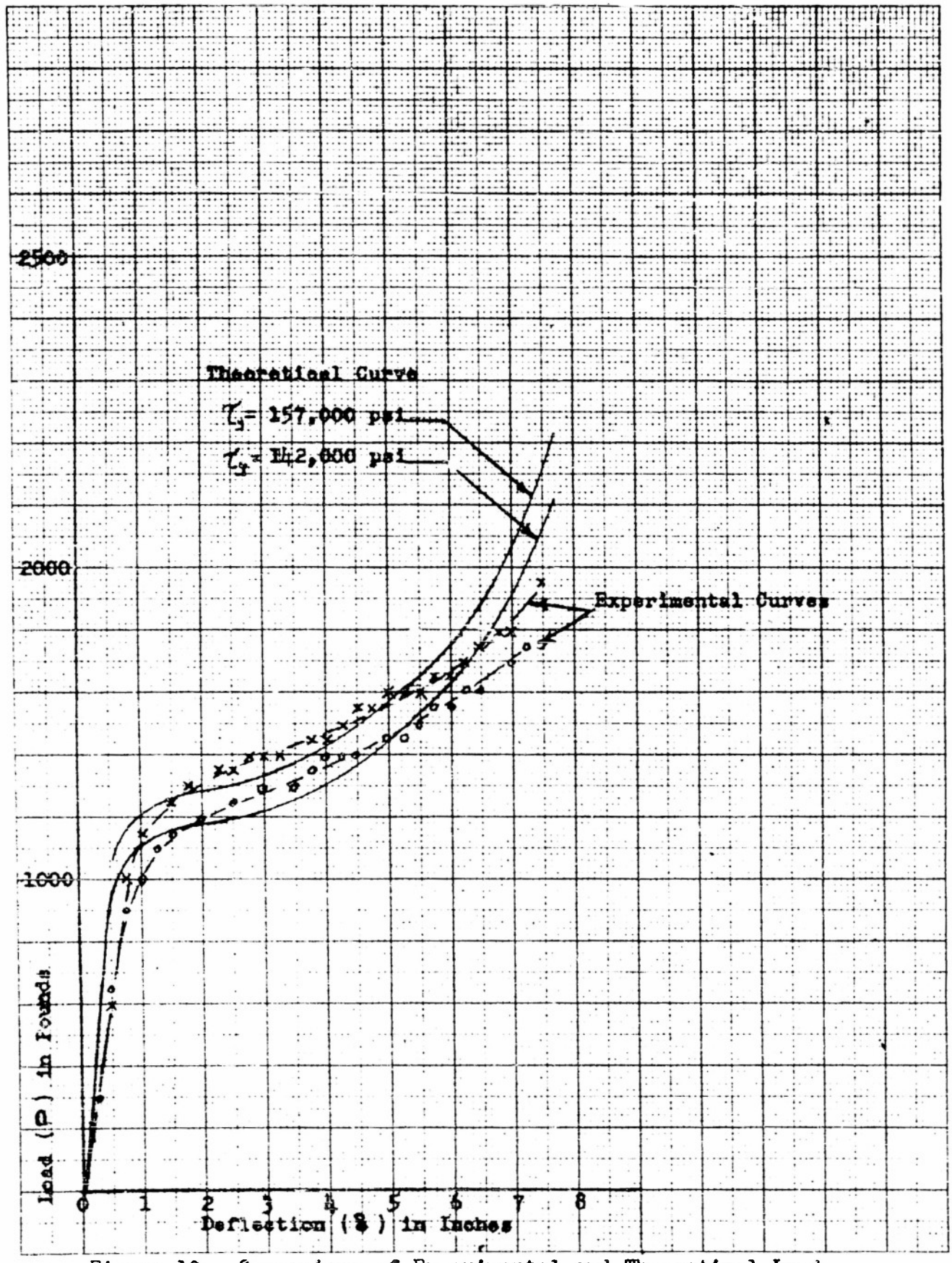

Figure 10. Comparison of Experimental and Theoretical Load-Deflection Curves of the Size 2 Extendible Element

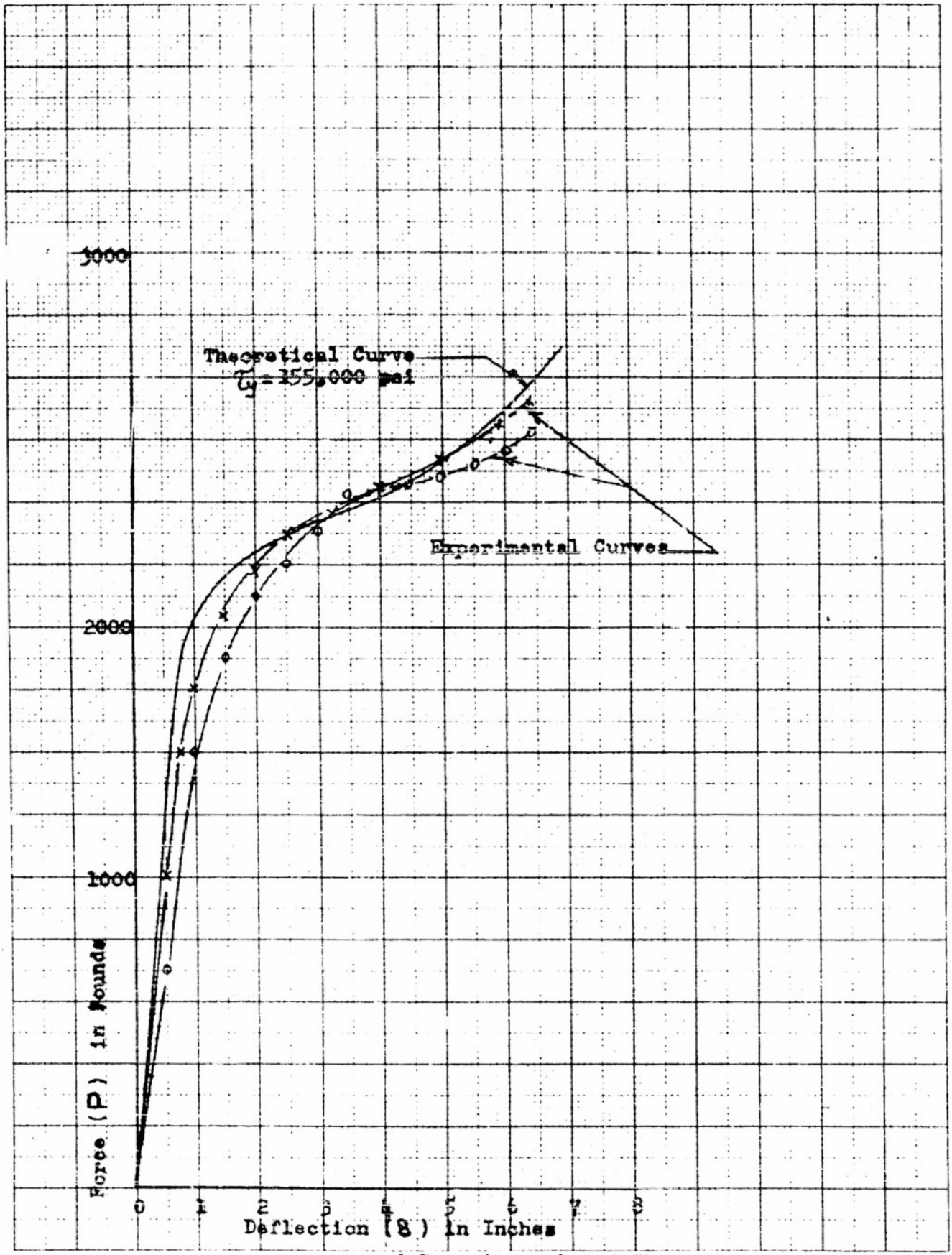

Figure 11. Comparison of Experimental and Theoretical Load-Deflection Curves of the Size 3 Extendible Element

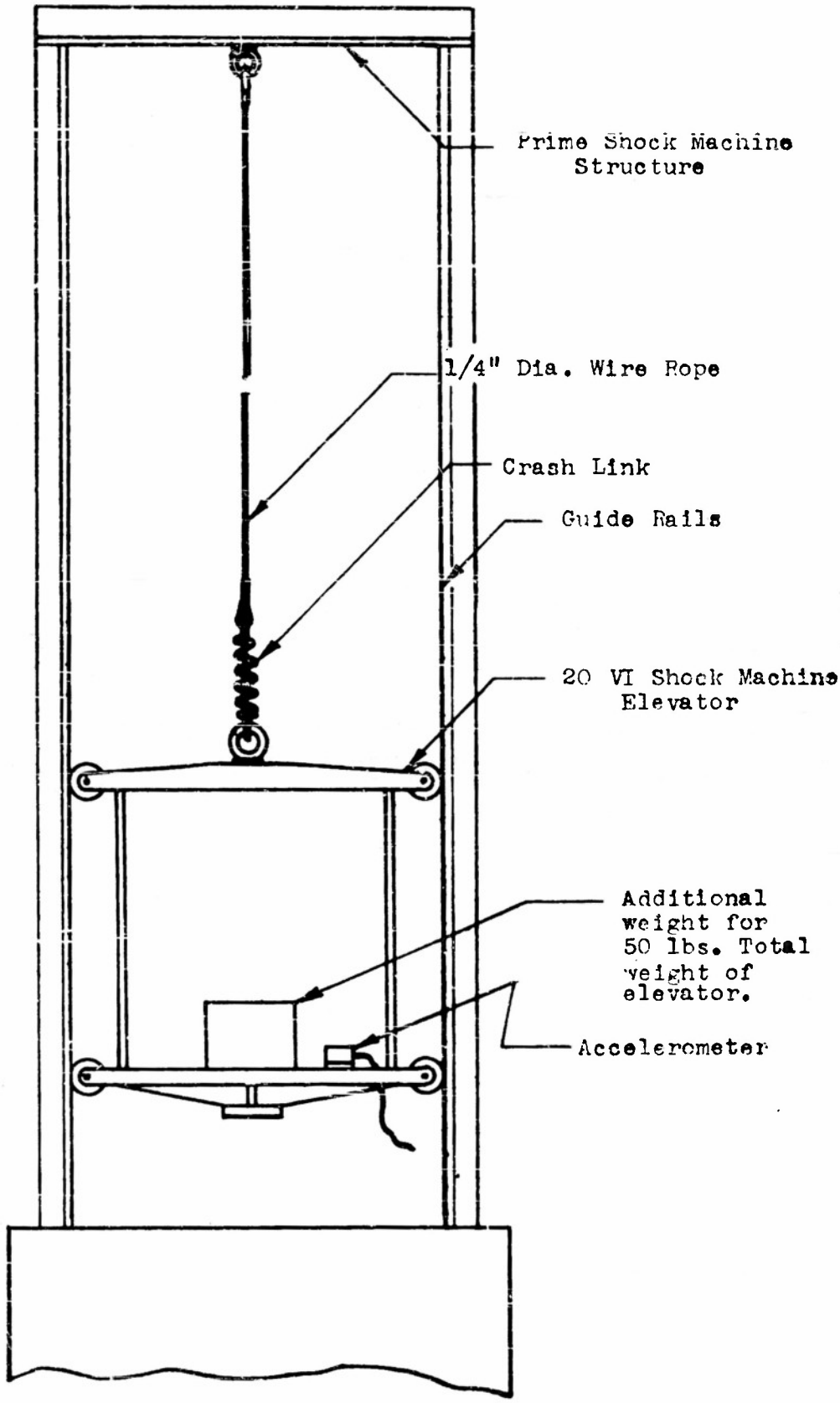

Figure 12. Drop Test Set-Up For Crash Link

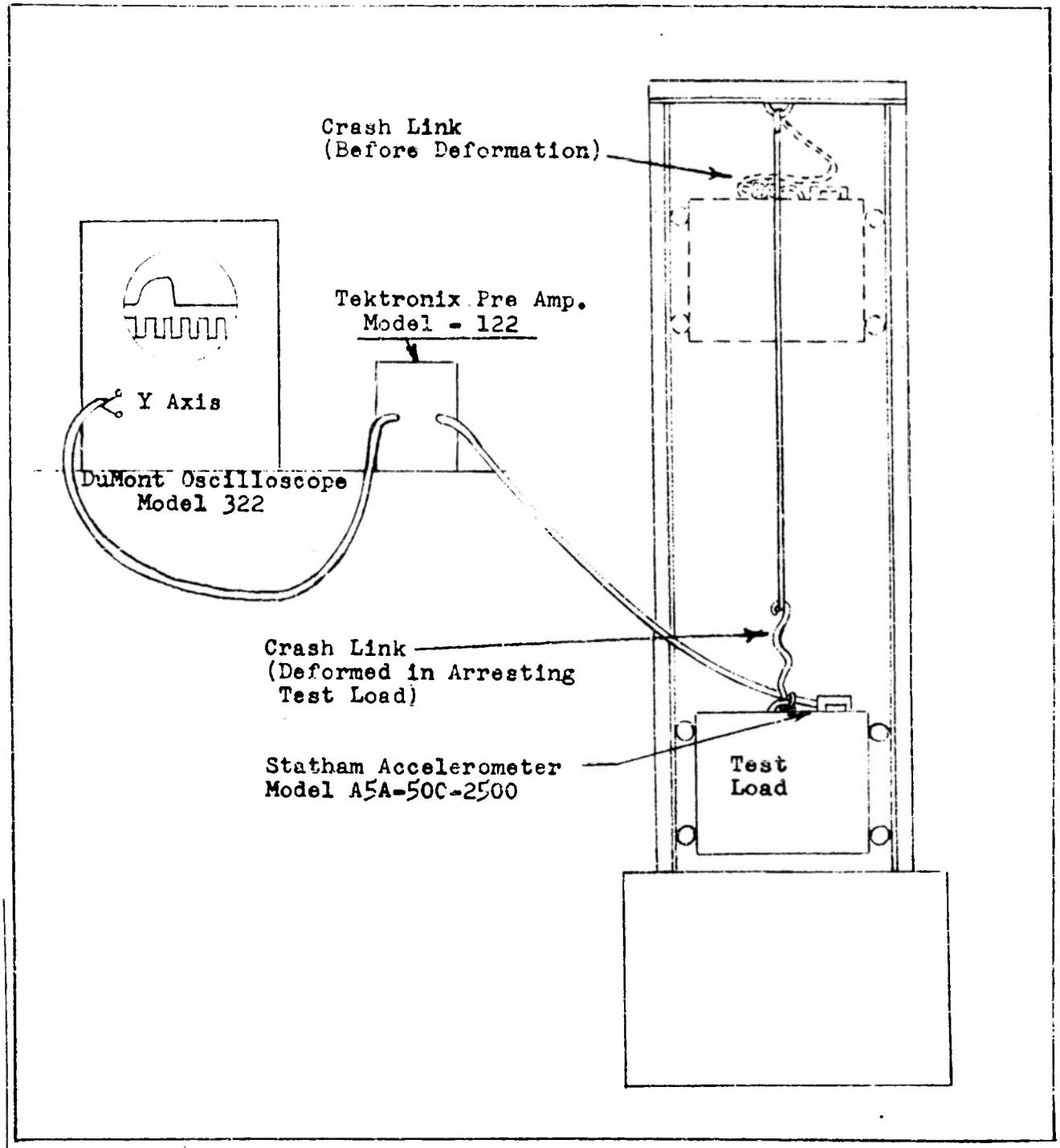

Figure 13. Instrumentation Used to Measure Dynamic Force Developed by the Crash Link in Arresting Dummy Equipment Load

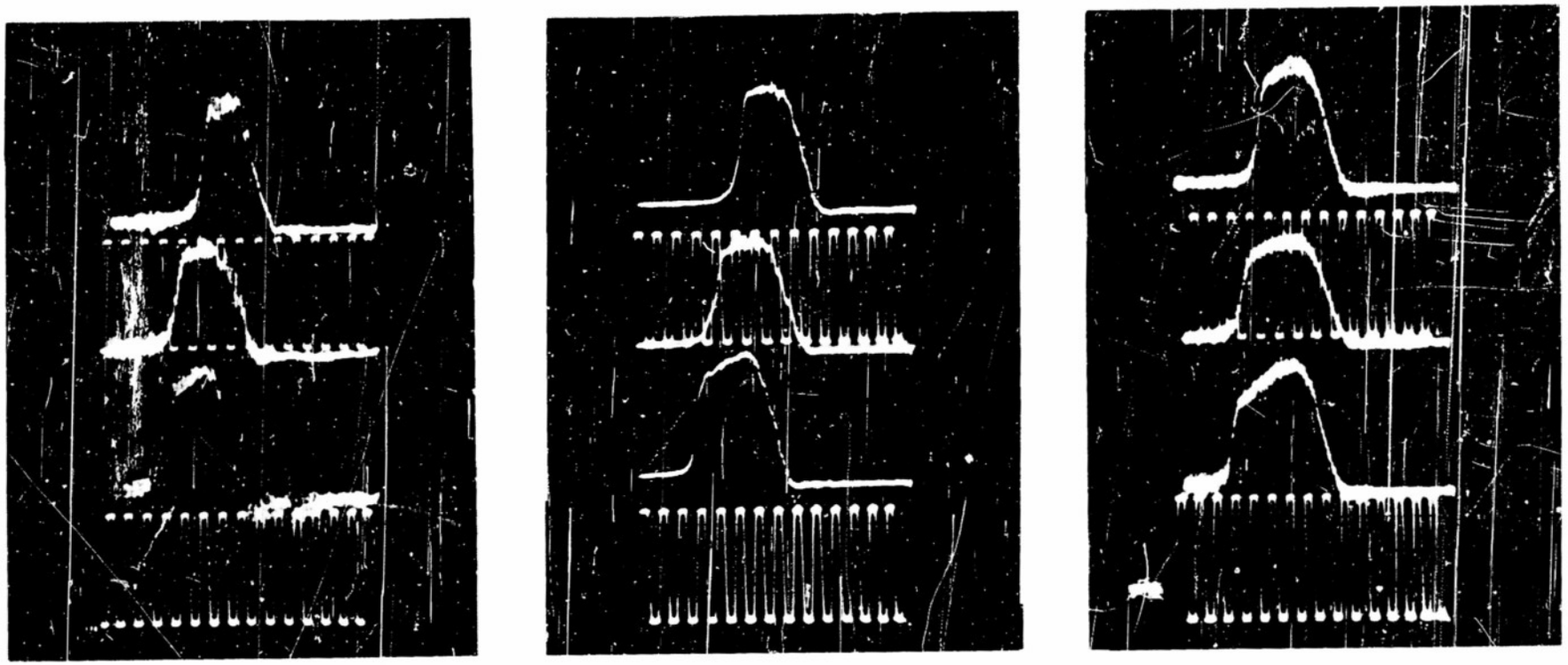

Size 1 Size 2 Size 3

Figure 14 Acceleration Versus Time Oscillograms of the Three Sizes of Extendible Elements

Upper Trace of Each Oscillogram - First Five Foot Drop of Link No. 1
Middle Trace of Each Oscillogram - Second Five Foot Drop of Link No. 1
Lower Trace of Each Oscillogram - Nine Foot Drop of Link No. 2
Calibration Traces: 60 cps; 15g Peak to Peak

DISTRIBUTION LIST

Copies	Activities at Wright-Patterson Air Force Base
5	DSC-SA
2	WCOSI3
9	WCREO-2
1	WCOSI(for transmittal to Office of Technical Services, Dept. of Commerce, Washington 25, D. C.)
1	WCLET Attn: D.C. Kennard
1	WCLNI
1	WCLNQ Attn: C.W. McDowell
1	WCLRE-1 Attn: M.J. McPeek
1	WCLRI
1	WCRTO-5
1	WCOSI (for transmittal to the Rand Corp., 1700 Main St., Santa Monica, Cal.)
3	WCOSR (for possible foreign release)
1	WCSAR
1	WCLFA-3

Other Department of Defense Agencies

Air Force

Copies	
3	Commander Air Force Cambridge Research Center Attn: Documents Unit, CRQST-2 230 Albany Street Cambridge 39, Massachusetts
1	Commander Rome Air Development Center Attn: RCRES-4C Griffiss Air Force Base Rome, New York
1	Commander AF Missile Test Center Patrick Air Force Base Cocoa, Florida
1	Director Air University Library Maxwell Air Force Base, Alabama

Copies	Other Department of Defense Agencies
1	Chief Technical Library Office of Asst. Secretary of Defense (R&D) Room 3E 1065, The Pentagon Washington 25, D. C.
1	Air Force Development Field Representative Code 1010 Naval Research Laboratory Washington 25, D. C.
1	Chief European Office Air Research & Development Command Shell Building 60 Rue Ravenstein Brussels, Belgium Via International Mail

Army

Copies	
1	Commanding General Redstone Arsenal Attn: Technical Library-EC Huntsville, Alabama
1	Commanding General Signal Corps Engineering Labs. Attn: Technical Documents Center Evans Signal Lab Area, Bldg. 27 Belmar, New Jersey

Navy

Copies	
1	Chief Bureau of Aeronautics Electronics Division Material Coordination Unit Navy Department Washington 25, D. C.
1	Chief Bureau of Aeronautics Attn: Technical Data Division TD-414 Navy Department Washington 25, D. C.

Other Department of Defense

Copies	Agencies
1	Chief Bureau of Ships Code 816 Navy Department Washington 25, D. C.
1	U.S. Navy Electronics Laboratory Attn: Mr. A.H. Attebury Code 733 San Diego 52, California

Miscellaneous

1	National Bureau of Standards Div. 12.1 Miniaturization Laboratory Attn: Gustave Shapiro Washington 25, D. C.
5	The Barry Corporation Attn: Richard D. Cavanaugh 700 Pleasant Street Watertown 72, Massachusetts